Cancer Science
The official journal of the Japanese Cancer Association

Hepatocellular carcinoma development induced by conditional β-catenin activation in *Lkb1*$^{+/-}$ mice

Hiroyuki Miyoshi,[1,4] Atsuko Deguchi,[1] Masayuki Nakau,[2] Yasushi Kojima,[1] Akira Mori,[2] Masanobu Oshima,[1,5] Masahiro Aoki[1] and Makoto Mark Taketo[1,3]

[1]Department of Pharmacology, Kyoto University Graduate School of Medicine; [2]Department of Surgery, Graduate School of Medicine, Kyoto University, Kyoto, Japan

(Received June 05, 2009/Revised July 04, 2009/Accepted July 06, 2009/Online publication August 4, 2009)

The development of hepatocellular carcinomas (HCC) appears to be a multistep process that takes several decades in humans. However, the identities of specific gene alterations and their contribution to HCC pathogenesis remain poorly understood. We previously reported that *Lkb1*$^{+/-}$ mice spontaneously develop multiple hepatic nodular foci (NdFc) followed by HCC, and that the conditional activation of β-catenin in *Catnb*$^{lox(ex3)}$ mouse livers alone does not cause tumor formation. We show here that the conditional activation of β-catenin accelerates HCC development in *Catnb*$^{+/lox(ex3)}$*Lkb1*$^{+/-}$ compound mutant mice, affecting displastic hepatocytes in NdFc that suffered LOH at the *Lkb1* locus. We further show that β-catnin activation provides HCC with a growth advantage as well as transplantability. These results suggest that the loss of *Lkb1* contributes to the formation of dysplastic NdFc, and that Wnt signaling activation is involved in ensuing progression toward HCC. A combination of these sequential changes can be a practical model for a subset of human HCC. (*Cancer Sci* 2009; 100: 2046–2053)

Peutz–Jeghers syndrome (PJS) is an autosomal dominant disease characterized by gastrointestinal hamartoma and mucocutaneous pigmentation as well as the increased risk of cancer.[1,2] The positional cloning studies on chromosome 19p13.3 identified mutations in *LKB1* responsible for PJS.[3,4] LKB1 is a serine/threonine kinase that phosphorylates and activates 14 kinases, including AMP-activated protein kinase (AMPK) and microtubule-associated protein/microtubule affinity-regulating kinases (MARK).[5] Recent studies have revealed that LKB1 mediates energy-dependent suppression of the mammalian target of rapamycin (mTOR) pathway via AMPK,[6] and that LKB1 suppresses tubulin polymerization by activating MARK–microtubule-associated protein signaling.[7]

We previously reported that *Lkb1*$^{+/-}$ mice develop gastrointestinal hamartomas that have similar histopathology to those in human PJS.[8] In addition, they developed multiple small nodular foci (NdFc) in the liver after 30 weeks of age, and HCC after 40 weeks of age.[9] NdFc consist of dysplastic and proliferative hepatocytes, suggesting that HCC in *Lkb1*$^{+/-}$ mice originate from these lesions.[9] *LKB1* mutations have been identified not only in PJS patients but also in sporadic cancers.[10] Although the liver malignancy in PJS patients has been rarely reported, LKB1 is implicated in the pathogenesis of human HCC. A HCC cell line (BEL9204) and an immortalized hepatocyte line (TPH1) were found to bear homozygous deletions of the *LKB1* gene,[11] and 1 of the 80 primary HCC examined had a point mutation in the *LKB1* kinase domain.[12] These results suggest that LKB1 deficiency may underlie a subset of human HCC.

Wnt signaling activation is a frequent change in HCC as well as in other cancers.[13] Upon activation, the adenomatous polyposis coli (APC)–axin–glycogen synthase kinase 3β (GSK3β) complex is unable to phosphorylate β-catenin, which results in the stabilization of β-catenin followed by the activation of T-cell factor (TCF)/lymphoid enhancer factor (LEF)-dependent transcription. β-Catenin mutations in GSK3β phosphorylation sites have been identified in human, mouse, and rat HCC.[14–16] We previously constructed *Catnb*$^{lox(ex3)}$ mice, in which exon 3 of the gene encoding β-catenin was sandwiched by two *loxP* sites.[17] Liver-specific recombination by Cre recombinase resulted in hepatomegaly with mitochondrial swelling in hepatocytes.[18] However, no neoplastic changes of hepatocytes were observed as a result of the activation of β-catenin for up to 6 months following Cre induction by the recombinant adenovirus (AdCMV-*cre*). On the other hand, another Wnt signaling activation model was reported in which the *Apc* gene was conditionally disrupted by Cre recombinase.[19] Although these mice developed HCC and preneoplastic foci, it took 8–9 months after Cre induction, and latency was too long despite efficient recombination in approximately half of all hepatocytes. These results suggest that Wnt signaling activation alone is insufficient for hepatocarcinogenesis, in contrast to the extensive polyposis in the intestines of *Catnb*$^{lox(ex3)}$*Krt19*^{cre} and *Apc*$^{\Delta 716}$ mice.[17,20]

It appears that single gene mutations are not sufficient to cause HCC, as various gene mutations and chromosomal aberrations are accumulated during multistep hepatocarcinogenesis in humans.[21] To investigate the possible cooperation between the loss of LKB1 and the activation of β-catenin in HCC development, we introduced the *Catnb*$^{lox(ex3)}$ allele to *Lkb1*$^{+/-}$ mice and conditionally activated Wnt signaling in their livers by AdCMV-*cre* infection.

Materials and Methods

Mice. Construction of *Lkb1* knockout and *Catnb*$^{lox(ex3)}$ mice has been described previously.[8,17] We used only males due to the low incidence of NdFc and HCC in female *Lkb1*$^{+/-}$ mice, as previously reported.[9] For the adenoviral infection study, we generated *Catnb*$^{lox(ex3)}$, *Lkb1*$^{+/-}$, and the compound mutant mice by intercrossing *Catnb*$^{lox(ex3)}$ and *Lkb1*$^{+/-}$ mice. We further used age-matched *Lkb1*$^{+/-}$ mice to obtain additional NdFc and HCC samples for the following analyses. To inoculate and maintain transplanted HCC, we purchased C.B-17/lcr-*scid/scid* (Fox Chase SCID) and BALB/cA-*nu/nu* (Nude) mice from CLEA Japan (Tokyo, Japan). All animal experiments were approved by the Animal Care and Use Committee of Kyoto University.

[3]To whom correspondence should be addressed.
E-mail: taketo@mfour.med.kyoto-u.ac.jp
[4]Present address: Department of Pathology and Immunology, Washington University School of Medicine, St Louis, MO, USA.
[5]Present address: Division of Genetics, Cancer Research Institute, Kanazawa University, Kanazawa, Japan.

doi: 10.1111/j.1349-7006.2009.01284.x

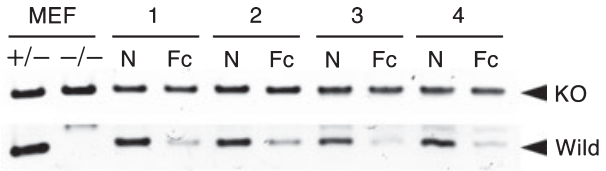

Fig. 1. Loss of intact *Lkb1* allele in preneoplastic nodular foci (NdFc) of *Lkb1*$^{+/-}$ mice. A genomic PCR analysis for *Lkb1* targeted alleles (KO) and wild-type alleles (Wild) was carried out using template DNA from four pairs of NdFc (Fc) and adjacent normal tissues (N). As a control, a pair of fibroblast (MEF) preparations from *Lkb1*$^{+/-}$ and *Lkb1*$^{-/-}$ embryos was also examined.

LOH analysis. DNA extraction from paraffin-embedded sections and genomic PCR for the targeted and wild-type *Lkb1* alleles were carried out as described previously.[22]

Antibodies. Antibodies for GS (FL-373), p27 (C-19), cyclin A (H-432), cyclin D1 (M-20), cyclin E (M-20; Santa Cruz Biotechnology, Santa Cruz, CA, USA), human LKB1 (sheep polyclonal), mouse LKB1 (rabbit polyclonal), c-Myc (rabbit polyclonal; Upstate, Charlottesville, VA, USA), β-catenin (rabbit polyclonal; Sigma, St Louis, MO, USA), Ki-67 (TEC3; Dako, Glostrup, Denmark), and GAPDH (6C5; Ambion, Austin, TX, USA) were purchased from commercial sources.

Western blotting analysis. Sample preparations from tissues, electrophoresis, and transfer to nitrocellulose membrane were carried out as described previously.[8,9] Membranes were incubated with primary antibodies diluted in Blocking One (Nacalai Tesque, Kyoto, Japan) at 4°C overnight and secondary antibodies at room temperature for 30 min. Immobilon Western HRP Chemiluminescent Substrate (Millipore, Bedford, MA, USA) was used to detect the specific signals. Band intensity was visualized and quantified using Image Gauge application software (Fujifilm, Tokyo, Japan).

Histopathological analysis. Preparation of histological specimens and immunostaining were carried out as described previously.[8,9] Antigen retrieval by microwave was carried out in 10 mM citrate buffer (pH 6.0) before incubation with the primary antibody for Ki-67. Brightfield images were captured and analyzed with Nikon ECLIPSE E800 (Tokyo, Japan) and Adobe Photoshop software (San Jose, CA, USA).

Microarray analysis. Total RNA was extracted from tumors by RNeasy Plus (Qiagen, Valencia, CA, USA). Cy3- and Cy5-labeled amplified antisense RNA (aRNA) was synthesized by the Amino Allyl Message Amp II aRNA Amplification Kit (Ambion). A mixture of two-colored probes was competitively hybridized to the arrays spotted with the mouse oligo library (Sigma). After washing, arrays were dried and scanned by the microarray scanner system G2565BA (Agilent Technologies, Palo Alto, CA, USA). The data were analyzed using Feature Extraction software (Agilent Technologies).

RT-PCR. Total RNA was prepared from tissues using ISOGEN solution (Nippon Gene, Tokyo, Japan), and cDNA was synthesized with SuperScript III reverse transcriptase (Invitrogen, Carlsbad, CA, USA). Primer sequences for specific gene amplification are shown in Table S1.

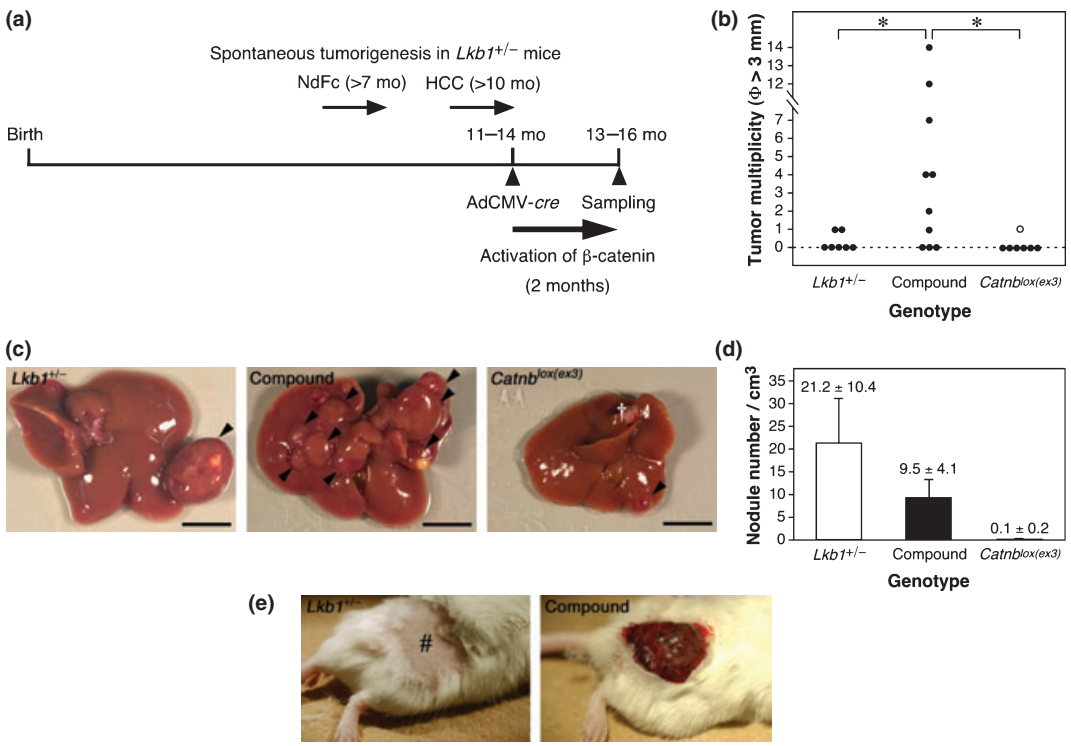

Fig. 2. Acceleration of hepatic tumorigenesis by activation of β-catenin in *Catnb*$^{+/lox(ex3)}$*Lkb1*$^{+/-}$ compound mutant mice. (a) Experimental schedule for this study. All animals in the crossing experiment were infected with AdCMV-*cre* at the ages shown in months (mo). (b) Tumor multiplicities 2 months after AdCMV-*cre* infection. Tumors larger than 3 mm in diameter visible on the liver surface were counted under a dissection microscope. Statistical analysis was carried out with Mann–Whitney's *U*-test. *$P < 0.05$. One tumor that was found in a *Catnb*$^{lox(ex3)}$ mouse (open circle) was a NdFc histologically. (c) Gross appearance of representative liver tumors (arrowheads). †Connective tissue associating with vessels. Scale bars = 1 cm. (d) Estimated numbers of microscopic NdFc in the liver. The number of microscopic nodules larger than 200 μm in diameter per cm^3 liver was calculated as described.[23] Data are expressed as the mean with SD. The difference of average NdFc numbers between *Lkb1*$^{+/-}$ and the compound mutant mice was not statistically significant by Student's *t*-test. (e) SCID mice inoculated with primary tumors from a *Lkb1*$^{+/-}$ mouse (left) and a compound mutant mouse (right). Photographs were taken 2 months after transplantation. #Tumor inoculation site.

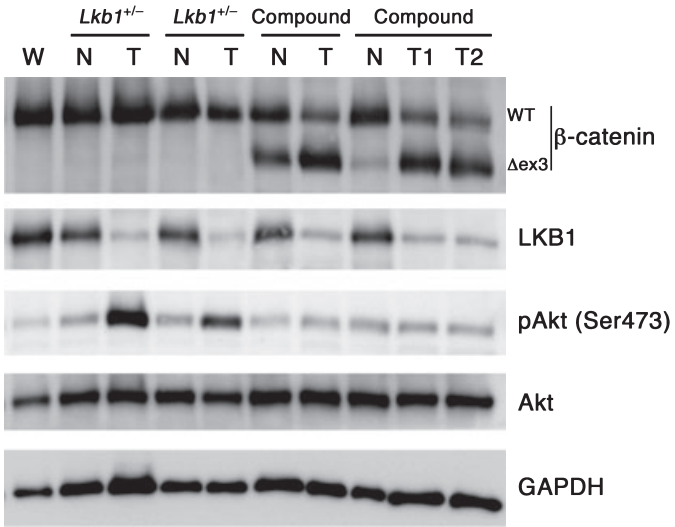

Fig. 3. Concomitant changes of LKB1 and β-catenin expression in liver lesions. Western blotting analysis for β-catenin (WT, wild-type; Δex3, stabilized mutant), LKB1, phospho-Akt (Ser473), and total Akt with GAPDH control is shown. A wild-type liver (W), and pairs of tumor (T) and adjacent normal tissue (N) from two $Lkb1^{+/-}$ and two compound mutant mice were analyzed.

Table 1. Upregulated and downregulated genes in hepatocellular carcinomas (HCC) with the activation of β-catenin

Category and symbol	Fold change†		Reference‡
	C1/L1	C2/L2	
Transporter			
Slco1b2	66.15	67.09	
Slc10a1	18.72	20.20	
Slc21a5	8.38	6.01	
Slc1a2	7.71	8.59	(24)
Rhbg	6.68	6.10	(24,25)
Slc16a7	4.24	6.99	(24)
Abcc1a	0.23	0.24	
P450			
Cyp2e1	23.43	19.32	(25)
Cyp2c39	11.57	17.36	
Cyp2c29	8.96	10.02	(25)
Cyp1a2	4.59	17.62	(25)
Cyp27a1	4.24	10.14	
Cyp2f2	0.14	0.05	(24)
Amino acid metabolism			
Oat	8.97	7.98	(25,26)
Asns	7.07	7.52	
Hal	0.21	0.04	(24)
Sds	0.22	0.09	(24)
Secretory protein			
Tgn	20.12	19.37	
Spp2	14.46	7.25	
Igfbp2	10.57	4.46	
Lect2	8.86	17.02	(27)
Other			
Lgr5	10.80	8.48	(24,28)
2310007H09Rik	9.47	6.75	(24)
Avpr1a	7.69	11.85	(24)
Raet1c	0.05	0.08	

†Fold changes in the transplanted HCC of the compound mutant mice (C1 or C2) compared with those of $Lkb1^{+/-}$ mice (L1 or L2) are shown.
‡References are shown, in which the correlation with the Wnt signaling is reported.

Human HCC samples. Surgical specimens of the primary HCC were collected, with informed consent, upon surgery at Kyoto University Hospital with the protocol approved by the Ethics Committee of Kyoto University.

Results

Loss of *Lkb1* heterozygosity causes dysplastic NdFc in the liver of $Lkb1^{+/-}$ mice. We previously reported that all HCC in the $Lkb1^{+/-}$ mice tested had lost expression of LKB1 protein due to the loss of *Lkb1* heterozygosity.[9] To investigate whether dysplastic cells in the NdFc of $Lkb1^{+/-}$ mice also show LOH at the *Lkb1* locus, we carried out PCR using genomic DNA samples from the NdFc and adjacent normal tissues, separated by laser microdissection. In all of the 14 pairs of samples, the band intensities for the wild-type allele were significantly weaker in the NdFc than in the adjacent normal tissues (Fig. 1 and data not shown), suggesting that loss of LKB1 expression by LOH at the *Lkb1* locus is likely an initiating event of hepatocarcinogenesis in $Lkb1^{+/-}$ mice.

Activation of β-catenin accelerates hepatocarcinogenesis in $Catnb^{+/lox(ex3)}Lkb1^{+/-}$ compound mutant mice. To investigate possible cooperation between the loss of LKB1 and the activation of β-catenin in HCC development, we introduced a floxed stabilizing β-catenin gene (i.e. $Catnb^{lox(ex3)}$ allele) into the $Lkb1^{+/-}$ mice and generated $Catnb^{+/lox(ex3)}Lkb1^{+/-}$ mice (hereafter compound mutant mice). Expression of β-catenin$^{\Delta ex3}$, a stabilized form lacking the GSK3β phosphorylation sites, can be induced in hepatocytes of these mice by Cre-mediated excision of exon 3 from the $Catnb^{lox(ex3)}$ allele through intravenous injection of the Cre-expressing adenovirus AdCMV-*cre*.[17] Because high multiplicity of infection of the hepatocytes with AdCMV-*cre* causes fatal Wnt signaling,[18,19] we adjusted the adenovirus titer to 2×10^7 pfu per mouse, a dose that should activate Wnt signaling only in ~10% of the hepatocytes (Fig. S1). $Catnb^{+/lox(ex3)}$ (hereafter $Catnb^{lox(ex3)}$ mice), $Lkb1^{+/-}$, and their compound mutant mice were infected with AdCMV-*cre* at 11–14 months of age. They were euthanized 2 months post-infection and their livers were examined (Fig. 2a). Two of seven $Lkb1^{+/-}$ mice developed single detectable tumors on the liver surface, whereas only one of seven $Catnb^{lox(ex3)}$ mice had a tumor that was diagnosed as NdFc histologically (Fig. 2b,c). On the other hand, the compound mutant mice developed multiple tumors, ranging from 0 to 14 per animal, that were visible on the liver surface. These results suggest that the activation of β-catenin accelerates hepatocarcinogenesis in $Lkb1^{+/-}$ mice. In contrast, no macroscopic liver tumors were found when younger compound mutant mice at 2 months of age were Wnt-activated in the same manner (data not shown). Considering the long latency of hepatocarcinogenesis in $Lkb1^{+/-}$ mice (Fig. 2a), it was likely that liver tumors in the compound mutant mice derived from microscopic NdFc rather than from normal hepatocytes. It was also possible, however, that activation of β-catenin increased the number of NdFc in the aged compound mutant mice, which could have accelerated the liver tumor development by expanding the NdFc population. To test this possibility, we estimated the number of microscopic foci per unit volume of the liver using a mathematical formula.[23] However, the number of nodules estimated in the compound mutant mice was even lower than that in the $Lkb1^{+/-}$ mice (Fig. 2d), excluding the possibility that activation of β-catenin was involved in the early events of hepatocarcinogenesis in the compound mutant mice.

HCC in the compound mutant mice have higher transplantability than those in $Lkb1^{+/-}$ mice. To test the effect of the activation of β-catenin on transplantability of the HCC, we subcutaneously inoculated the primary HCC clumps from the $Lkb1^{+/-}$ and compound mutant mice into immunocompromised

doi: 10.1111/j.1349-7006.2009.01284.x

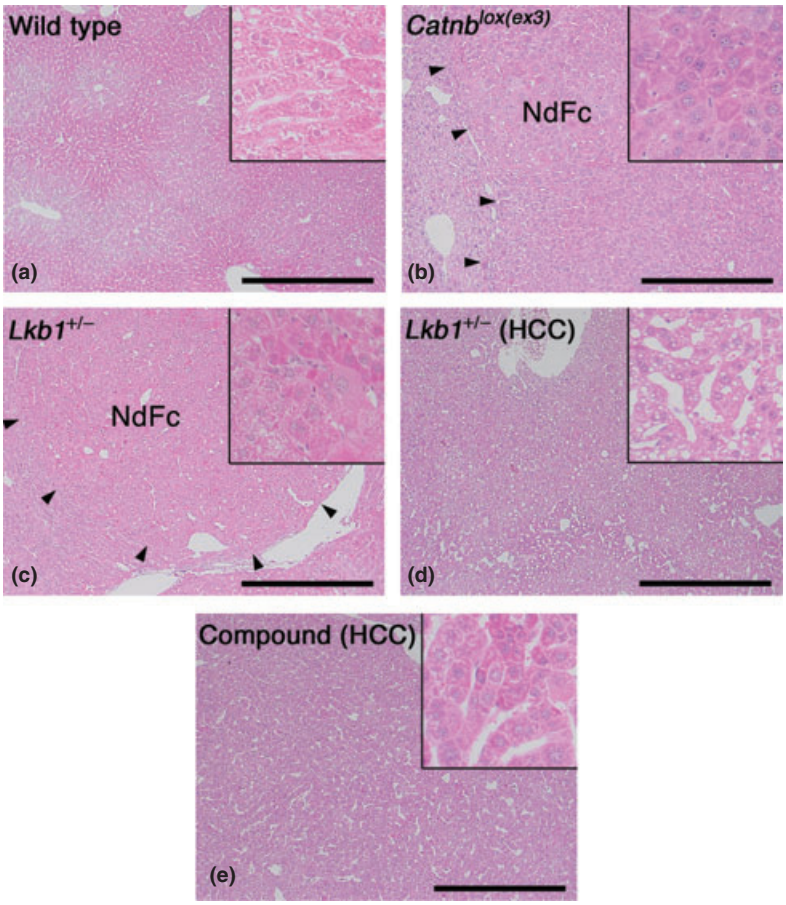

Fig. 4. Minimal effects of activated β-catenin on histopathology of hepatocellular carcinomas (HCC). HE stains of (a) wild-type liver, (b) a nodular focus in a *Catnb*$^{lox(ex3)}$ mouse, (c) a nodular focus in a *Lkb1*$^{+/-}$ mouse, (d) a HCC in a *Lkb1*$^{+/-}$ mouse, and (e) a HCC in a compound mutant mouse. Insets are at a higher magnification. Arrowheads show the boundary between normal and tumor tissues. Scale bars = 500 μm.

SCID mice. Although no growths were obtained in 2 months from any of the four HCC derived from *Lkb1*$^{+/-}$ mice, two of three HCC from the compound mutant mice formed tumors of >1 cm in diameter (Fig. 2e). After long-term incubation (>6 months), we could establish two transplantable HCC lines from the *Lkb1*$^{+/-}$ mice as well. These results indicate that activated β-catenin increases the transplantability of HCC in immunocompromised mice.

Concomitant loss of LKB1 and Wnt signal activation are reflected in the transcriptomes of HCC of compound mutant mice. We determined the expression levels of LKB1 and β-catenin protein in *Lkb1*$^{+/-}$ and the compound mutant mouse livers (Fig. 3). HCC of *Lkb1*$^{+/-}$ mice expressed a similar level of β-catenin to non-tumor tissues, suggesting that Wnt signaling was not activated in these tumors. Truncated β-catenin was detected in both HCC and normal adjacent tissues of the compound mutant mice (Fig. 3). We found that all HCC in the compound mutant mice lacked expression of LKB1 as in *Lkb1*$^{+/-}$ mice, and PCR analysis using the laser microdissection samples from those HCC showed that they had undergone LOH at *Lkb1* loci (data not shown). Interestingly, HCC in *Lkb1*$^{+/-}$ mice showed Akt activation whereas the compound mutant mice did not. These results collectively suggest that the activation of β-catenin promotes tumor progression in the dysplastic hepatocytes that had lost LKB1, through a mechanism distinct from *Lkb1*$^{+/-}$ mice.

To obtain insights into the effects of β-catenin activation on the transcriptome of HCC, we next compared the gene expression profiles of transplanted HCC (C1 and C2 from the compound mutant mice and L1 and L2 derived from the *Lkb1*$^{+/-}$ mice) for 22 056 mRNA species, using two sets of microarray data (C1 vs L1 and C2 vs L2). We listed genes whose expression levels changed more than four-fold in both assays, and found that 36 genes were upregulated whereas 24 genes downregulated in C1 and C2 compared with L1 and L2 (Tables S2 and S3, respectively). Table 1 summarizes the representative genes that were upregulated and downregulated in transplants with the activation of β-catenin. We further picked up several upregulated genes from the list and confirmed the microarray data by RT-PCR using cDNA from transplanted tumor lines (Fig. S2). Although expression of glutamine synthetase (GS) was not upregulatad (Fig. S3 and data not shown), the list includes several targets of the Wnt–β-catenin signaling pathway such as *Oat*, *Lect2*, and *Lgr5*.[26–28] Therefore, we concluded that the canonical Wnt signaling pathway was activated in HCC of the compound mutant mice but not in those of *Lkb1*$^{+/-}$ mice.

HCC in *Lkb1*$^{+/-}$ and compound mutant mice have similar histological phenotypes. We next studied the histopathology of the liver lesions in the compound and simple mutant mice. Wild-type livers showed well-organized hepatic cords (Fig. 4a), whereas NdFc in *Lkb1*$^{+/-}$ mice and *Catnb*$^{lox(ex3)}$ mice were composed of large dysplastic hepatocytes lacking the cord structure (Fig. 4b,c). Most HCC found in either *Lkb1*$^{+/-}$ or the compound mutant mice were of the trabecular type, consisting of well-differentiated carcinoma cells that formed disorganized cord structures (Fig. 4d,e). Three of 17 HCC in the compound mutant mice also contained a gland-like structure (data not shown). Together with our previous report,[9] these results show that the histopathological features of HCC in the compound mice are similar to those observed frequently in *Lkb1*$^{+/-}$ mice.

Wnt signal activation increases growth rate in HCC. To assess the effects of Wnt signal activation on the liver lesions, we

immunostained proliferative cells for Ki-67 protein. It is expressed in all cycling cells,[29] and was found in the NdFc and HCC of *Lkb1*$^{+/-}$ mice, HCC of the compound mutant mice, and NdFc of *Catnb*$^{lox(ex3)}$ mice (Fig. 5a–d). The fraction of Ki-67-positive cells was ~20% in HCC of the compound mutant mice, which was significantly higher than in *Lkb1*$^{+/-}$ mice as well as in the NdFc of *Lkb1*$^{+/-}$ or *Catnb*$^{lox(ex3)}$ mice (Fig. 5e). A similar increase in growth rate was observed in the HCC transplanted from the compound mutant mice (C1 and C2) compared with those in the *Lkb1*$^{+/-}$ mice (L1 and L2) (Fig. 5f). These results suggest that the increase in the proliferating cell fraction contributes to the rapid HCC tumorigenesis after infection of the compound mutant mice with AdCMV-*cre*.

Roles of Wnt signal activation in cell cycle regulation. To investigate further what increases proliferating cells downstream of Wnt signaling, we analyzed the expression profile of cell cycle-regulating proteins in transplanted HCC (Fig. 6a). Interestingly, expression of cyclin E was upregulated in C1 and C2 compared with wild-type liver, and in L1 to a lesser extent, whereas the levels of cyclin A, cyclin D1, and c-Myc in C1 and C2 remained at similar levels to those in L1 and L2 except for robust cyclin D1 expression in L2. An inhibitor of cyclin E/cyclin dependent kinase (CDK) 2 complex, p27 was downregulated. To analyze cyclin E expression *in vivo*, we immunostained the protein in the primary HCC of *Lkb1*$^{+/-}$ and compound mutant mice. HCC in the compound mutant mice had significantly high levels of cyclin E, whereas those in *Lkb1*$^{+/-}$ mice rarely contained positively stained nuclei (Fig. 6b). However, a semiquantitative RT-PCR analysis showed that the *Ccne1* mRNA level was only marginally higher in the HCC of the compound mutant mice than those in *Lkb1*$^{+/-}$ mice (Fig. 6c). These results suggested that accumulation of cyclin E was mediated by post-transcriptional regulation.

Discussion

In the present study, we have developed a new mouse model for HCC by compound mutations in *Lkb1* and β-catenin (*Catnb*$^{+/lox(ex3)}$*Lkb1*$^{+/-}$). We have shown that cells in NdFc of the *Lkb1*$^{+/-}$ mice lack LKB1 expression because of LOH (Fig. 1), suggesting that loss of LKB1 can be responsible for early steps of hepatocarcinogenesis. Considering the low incidence and

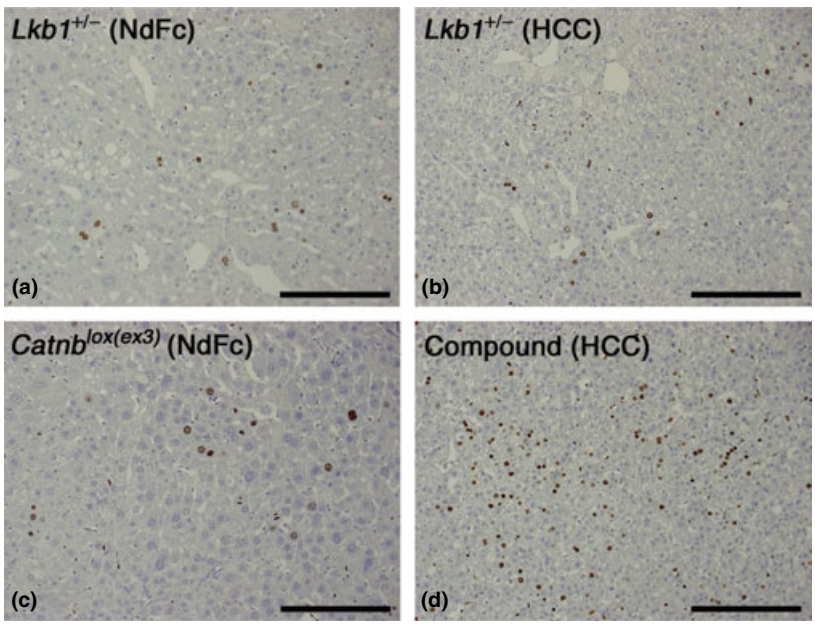

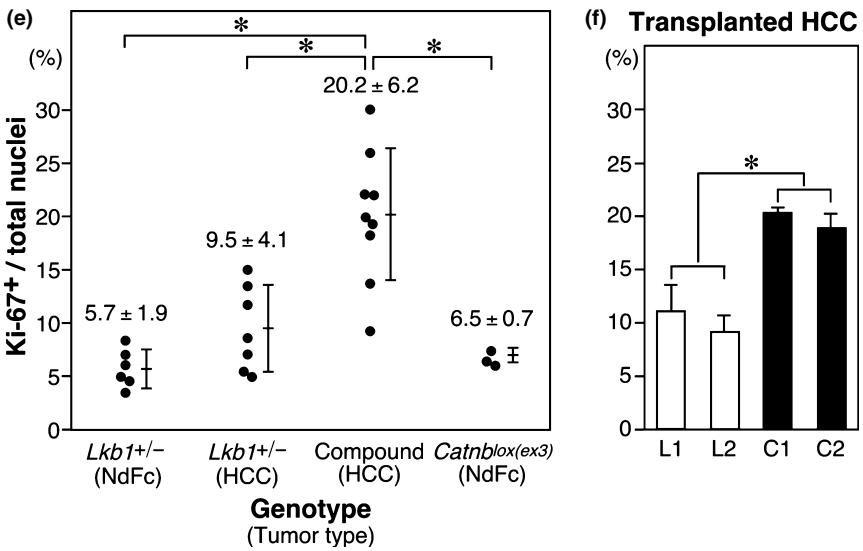

Fig. 5. Increase in the proliferating cell fraction in hepatocellular carcinomas (HCC) with activated β-catenin. Immunostaining for Ki-67 antigen in a (a) nodular focus and (b) HCC of *Lkb1*$^{+/-}$ mice, (c) a nodular focus of a *Catnb*$^{lox(ex3)}$ mouse, and (d) a HCC of a compound mutant mouse. Scale bars = 200 μm. (e) Proliferating cell indices in liver lesions. The fraction of proliferating cells (%) from each lesion was calculated from the number of Ki-67-positive and total nuclei. The mean rates with SD are shown. Data were analyzed statistically using Tukey's test. **P* < 0.05. (f) Proliferating cell indices in transplanted tumor lines. The mean rates with SD of four independent tumors are shown. Statistical analysis was by Student's *t*-test. **P* < 0.05.

doi: 10.1111/j.1349-7006.2009.01284.x

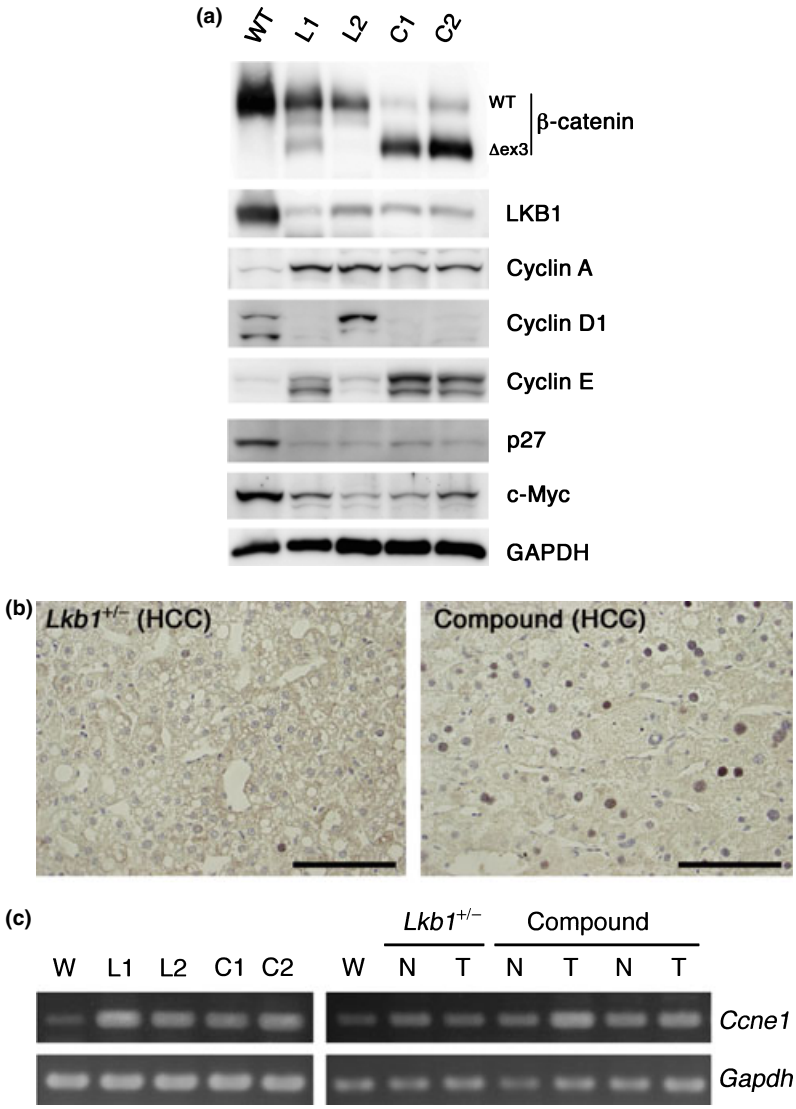

Fig. 6. Effects of Wnt signaling on cell cycle regulation. (a) Western blotting analysis of cell cycle-related proteins. Expression is also shown for β-catenin and LKB1 to confirm the genotypes of transplanted hepatocellular carcinomas (HCC). (b) Immunostaining for cyclin E in primary HCC of a *Lkb1*$^{+/-}$ (left) and compound mutant (right) mouse. Scale bars = 100 μm. (c) RT-PCR analysis for *Ccne1* in transplanted (left) and primary (right) HCC. Wild-type livers (W), transplanted HCC lines (L1, L2, C1, and C2), and pairs of the primary tumor (T) and adjacent normal tissue (N) were analyzed. Expression is shown for *Gapdh* mRNA as an internal control (lower panels).

multiplicity, and long latency to develop HCC in *Lkb1*$^{+/-}$ mice, additional genetic alterations are likely to be needed for the progression of NdFc to fully malignant HCC. In this new mouse model of HCC, multiple HCC developed when their livers were induced to express active β-catenin in *Lkb1*$^{+/-}$ mice at ~1 year of age, but not when induced at 2 months of age. Development of dysplastic NdFc in *Lkb1*$^{+/-}$ mice requires a long latency period (>30 weeks), and no foci can be found in these mice at 2 months of age. It is therefore plausible that HCC in the compound mutant mice arose as a result of β-catenin activation in a fraction of the dysplastic cells in the pre-formed NdFc. Thus, we propose a model where NdFc are initiated by the loss of *Lkb1*, through LOH, and a subset of such NdFc cells undergo activation of β-catenin, upon AdCMV-*cre* infection, and these cells progress further to form HCC.

HCC in the compound mutant mice contained a significantly larger number of proliferating cells than those in *Lkb1*$^{+/-}$ mice (20 vs 9.8% on average; Fig. 5e), which can explain the accelerated development of HCC in the compound mutant mice (Fig. 2c). In fact, these HCC with the activation of β-catenin rapidly grew when transplanted into immunocompromised mice (Fig. 2e). In the liver, Wnt signaling plays important roles in zonal expression of liver-specific genes along the portal-to-central axis,[30] including those for maturation of normal post-mitotic hepatocytes. On the other hand, we previously reported that co-expression of activated β-catenin and activated H-ras (H-rasG12V) in the hepatocytes led to HCC in mice at a high incidence, and that the activation of β-catenin in this model provoked proliferation and expansion of dysplastic lesions induced by the activated H-ras.[31] Growth advantage of HCC with activating mutations of β-catenin has also been demonstrated in other studies using human clinical samples or transgenic mouse models.[32–34] Accordingly, it is suggested that the Wnt signal activation increases the proliferation rate of the pre-formed dysplastic hepatocytes induced by other initiating events.

We have shown here that many of the genes known to be induced by Wnt signaling are upregulated in the compound mouse HCC. We found that cyclin E expression was upregulated in the compound mouse HCC, although expression levels remained unchanged in the compound mutant mice for c-Myc and cyclin D1, well-known direct targets of Wnt signaling.[35–37] Cyclin E promotes G_0/S transition through CDK-dependent and -independent mechanisms,[38,39] and ectopic cyclin E induction causes irregular entry of quiescent hepatocytes into the cell cycle.[40] It is therefore likely that cyclin E upregulation by Wnt signal activation promoted proliferation of HCC cells in the compound mutant mice, although the precise molecular mechanism of how Wnt signaling leads to cyclin E accumulation remains to be elucidated.

In conclusion, we have constructed a novel mouse model for multistep hepatocarcinogenesis by inducing two sequential genetic changes, where loss of LKB1 in hepatocytes triggers formation of NdFc, with the ensuing activation of β-catenin leading to the progression of NdFc into HCC. These model mice and their transplantable HCC should help elucidate the molecular mechanism of HCC progression at each step. We also believe that this model represents a subset of human HCC, where LKB1 and β-catenin mutations are involved (Fig. S4). Further clinical studies will estimate the contributions of the loss of LKB1 and activation to β-catenin on their pathogenesis and prognosis.

Acknowledgment

This work was supported by a Grant-in-Aid for Scientific Research from the Ministry of Education, Culture, Sports, Science, and Technology of Japan.

Disclosure Statement

None.

References

1 Giardiello FM, Welsh SB, Hamilton SR *et al.* Increased risk of cancer in the Peutz–Jeghers syndrome. *N Engl J Med* 1987; **316**: 1511–14.
2 Spigelman AD, Murday V, Phillips RK. Cancer and the Peutz–Jeghers syndrome. *Gut* 1989; **30**: 1588–90.
3 Hemminki A, Markie D, Tomlinson I *et al.* A serine/threonine kinase gene defective in Peutz–Jeghers syndrome. *Nature* 1998; **391**: 184–7.
4 Jenne DE, Reimann H, Nezu J *et al.* Peutz–Jeghers syndrome is caused by mutations in a novel serine threonine kinase. *Nat Genet* 1998; **18**: 38–43.
5 Alessi DR, Sakamoto K, Bayascas JR. LKB1-dependent signaling pathways. *Annu Rev Biochem* 2006; **75**: 137–63.
6 Shaw RJ, Bardeesy N, Manning BD *et al.* The LKB1 tumor suppressor negatively regulates mTOR signaling. *Cancer Cell* 2004; **6**: 91–9.
7 Kojima Y, Miyoshi H, Clevers HC, Oshima M, Aoki M, Taketo MM. Suppression of tubulin polymerization by the LKB1-microtubule-associated protein/microtubule affinity-regulating kinase signaling. *J Biol Chem* 2007; **282**: 23 532–40.
8 Miyoshi H, Nakau M, Ishikawa T, Seldin MF, Oshima M, Taketo MM. Gastrointestinal hamartomatous polyposis in *Lkb1* heterozygous knockout mice. *Cancer Res* 2002; **62**: 2261–6.
9 Nakau M, Miyoshi H, Seldin MF, Imamura M, Oshima M, Taketo MM. Hepatocellular carcinoma caused by loss of heterozygosity in *Lkb1* gene knockout mice. *Cancer Res* 2002; **62**: 4549–53.
10 Sanchez-Cespedes M. A role for *LKB1* gene in human cancer beyond the Peutz–Jeghers syndrome. *Oncogene* 2007; **26**: 7825–32.
11 Pineau P, Marchio A, Nagamori S, Seki S, Tiollais P, Dejean A. Homozygous deletion scanning in hepatobiliary tumor cell lines reveals alternative pathways for liver carcinogenesis. *Hepatology* 2003; **37**: 852–61.
12 Kim CJ, Cho YG, Park JY *et al.* Genetic analysis of the LKB1/STK11 gene in hepatocellular carcinomas. *Eur J Cancer* 2004; **40**: 136–41.
13 Polakis P. Wnt signaling and cancer. *Genes Dev* 2000; **14**: 1837–51.
14 de La Coste A, Romagnolo B, Billuart P *et al.* Somatic mutations of the β-catenin gene are frequent in mouse and human hepatocellular carcinomas. *Proc Natl Acad Sci USA* 1998; **95**: 8847–51.
15 Miyoshi Y, Iwao K, Nagasawa Y *et al.* Activation of the β-catenin gene in primary hepatocellular carcinomas by somatic alterations involving exon 3. *Cancer Res* 1998; **58**: 2524–7.
16 Pulling LC, Klinge DM, Belinsky SA. *p16*^{INK4a} and β-*catenin* alterations in rat liver tumors induced by NNK. *Carcinogenesis* 2001; **22**: 461–6.
17 Harada N, Tamai Y, Ishikawa T *et al.* Intestinal polyposis in mice with a dominant stable mutation of the beta-catenin gene. *EMBO J* 1999; **18**: 5931–42.
18 Harada N, Miyoshi H, Murai N *et al.* Lack of tumorigenesis in the mouse liver after adenovirus-mediated expression of a dominant stable mutant of β-catenin. *Cancer Res* 2002; **62**: 1971–7.
19 Colnot S, Decaens T, Niwa-Kawakita M *et al.* Liver-targeted disruption of Apc in mice activates beta-catenin signaling and leads to hepatocellular carcinomas. *Proc Natl Acad Sci USA* 2004; **101**: 17 216–21.
20 Oshima M, Oshima H, Kitagawa K, Kobayashi M, Itakura C, Taketo M. Loss of *Apc* heterozygosity and abnormal tissue building in nascent intestinal polyps in mice carrying a truncated *Apc* gene. *Proc Natl Acad Sci USA* 1995; **92**: 4482–6.
21 Thorgeirsson SS, Grisham JW. Molecular pathogenesis of human hepatocellular carcinoma. *Nat Genet* 2002; **31**: 339–46.
22 Takeda H, Miyoshi H, Kojima Y, Oshima M, Taketo MM. Accelerated onsets of gastric hamartomas and hepatic adenomas/carcinomas in *Lkb1*$^{+/-}$*p53*$^{-/-}$ compound mutant mice. *Oncogene* 2006; **25**: 1816–20.
23 Pugh TD, King JH, Koen H *et al.* Reliable stereological method for estimating the number of microscopic hepatocellular foci from their transections. *Cancer Res* 1983; **43**: 1261–8.
24 Stahl S, Ittrich C, Marx-Stoelting P *et al.* Genotype–phenotype relationships in hepatocellular tumors from mice and man. *Hepatology* 2005; **42**: 353–61.
25 Sekine S, Lan BY, Bedolli M, Feng S, Hebrok M. Liver-specific loss of β-catenin blocks glutamine synthesis pathway activity and cytochrome p450 expression in mice. *Hepatology* 2006; **43**: 817–25.
26 Cadoret A, Ovejero C, Terris B *et al.* New targets of β-catenin signaling in the liver are involved in the glutamine metabolism. *Oncogene* 2002; **21**: 8293–301.
27 Ovejero C, Cavard C, Périanin A *et al.* Identification of the leukocyte cell-derived chemotaxin 2 as a direct target gene of β-catenin in the liver. *Hepatology* 2004; **40**: 167–76.
28 Yamamoto Y, Sakamoto M, Fujii G *et al.* Overexpression of orphan G-protein-coupled receptor, *Gpr49*, in human hepatocellular carcinomas with β-catenin mutations. *Hepatology* 2003; **37**: 528–33.
29 Scholzen T, Gerdes J. The Ki-67 protein: from the known and the unknown. *J Cell Physiol* 2000; **182**: 311–22.
30 Benhamouche S, Decaens T, Godard C *et al.* Apc tumor suppressor gene is the ''zonation-keeper'' of mouse liver. *Dev Cell* 2006; **10**: 759–70.
31 Harada N, Oshima H, Katoh M, Tamai Y, Oshima M, Taketo MM. Hepatocarcinogenesis in mice with β-catenin and Ha-ras gene mutations. *Cancer Res* 2004; **64**: 48–54.
32 Nhieu JT, Renard CA, Wei Y, Cherqui D, Zafrani ES, Buendia MA. Nuclear accumulation of mutated β-catenin in hepatocellular carcinoma is associated with increased cell proliferation. *Am J Pathol* 1999; **155**: 702–10.
33 Calvisi DF, Ladu S, Factor VM, Thorgeirsson SS. Activation of β-catenin provides proliferative and invasive advantages in c-myc/TGF-α hepatocarcinogenesis promoted by phenobarbital. *Carcinogenesis* 2004; **25**: 901–8.
34 Calvisi DF, Conner EA, Ladu S, Lemmer ER, Factor VM, Thorgeirsson SS. Activation of the canonical Wnt/beta-catenin pathway confers growth advantages in c-Myc/E2F1 transgenic mouse model of liver cancer. *J Hepatol* 2005; **42**: 842–9.
35 He TC, Sparks AB, Rago C *et al.* Identification of c-MYC as a target of the APC pathway. *Science* 1998; **281**: 1509–12.
36 Tetsu O, McCormick F. β-Catenin regulates expression of cyclin D1 in colon carcinoma cells. *Nature* 1999; **398**: 422–6.
37 Shtutman M, Zhurinsky J, Simcha I *et al.* The cyclin D1 gene is a target of the β-catenin/LEF-1 pathway. *Proc Natl Acad Sci USA* 1999; **96**: 5522–7.
38 Hwang HC, Clurman BE. Cyclin E in normal and neoplastic cell cycles. *Oncogene* 2005; **24**: 2776–86.
39 Geng Y, Lee YM, Welcker M *et al.* Kinase-independent function of cyclin E. *Mol Cell* 2007; **25**: 127–39.
40 McEvoy JD, Kossatz U, Malek N, Singer JD. Constitutive turnover of cyclin E by Cul3 maintains quiescence. *Mol Cell Biol* 2007; **27**: 3651–66.

Supporting Information

Additional supporting information may be found in the online version of this article:

Fig. S1. Immunostainings for glutamine sysnthetase (GS) in (a) wild type and (b) *Catnb*$^{lox(ex3)}$ mouse livers. To determine the efficiency of adenoviral infection, we injected 2×10^7 pfu of AdCMV-*cre* into *Catnb*$^{lox(ex3)}$ mice and necropsied 1 week later. The activation of β-catenin was determined by immunostaining for GS, which is a target gene in hepatocytes.[26] Arrows point to GS-positive hepatocytes induced by AdCMV-*cre* infection. Arrowheads indicate expression of the endogenous GS around central veins (*). P, portal vein. Scale bars = 200 μm.

doi: 10.1111/j.1349-7006.2009.01284.x

Fig. S2. Levels of genes upregulated by activated β-catenin. RT-PCR results for representative genes are shown. Wild-type liver and transplanted HCC lines (L1, L2, C1, and C2) were analyzed.

Fig. S3. Expression of glutamine synthetase (GS) in a (a) wild-type liver, (b) nodular focus (NdFc) in a *Catnb*$^{lox(ex3)}$ mouse, (c) hepatocellular carcinoma (HCC) (T) in a *Lkb1*$^{+/-}$ mouse, and (d) HCC (T) in a compound mutant mouse. *, Central vein; P, portal vein. Scale bars = 500 μm.

Fig. S4. Expression of β-catenin and LKB1 in human hepatocellular carinomas (HCC). Western blotting analysis for β-catenin and LKB1 (arrowhead) with GAPDH control is shown. Five representative pairs of HCC (T) and adjacent tissue (N) are shown. Note β-catenin accumulation in patient 1, and its truncation in patient 3, accompanied by LKB1 downregulation.

Table S1. List of primer sequences for RT-PCR.

Tables S2 and S3. Upregulated and downregulated genes induced by activated β-catenin. The changes in mRNA levels between hepatocellular carcinoma (HCC) transplants from the compound mutant mice (C1 and C2) and *Lkb1*$^{+/-}$ mice (L1 and L2) were analyzed by DNA microarrays. The data are expressed as fold-changes (upregulated, C1/L1 and C2/L2; downregulated, L1/C1 and L2/C2).